Quasilinear saturation of the aperiodic ordinary mode streaming instability

A. Stockem Novo, P. H. Yoon, M. Lazar, R. Schlickeiser, S. Poedts, and J. Seough

Citation: Physics of Plasmas **22**, 092301 (2015); doi: 10.1063/1.4929852
View online: http://dx.doi.org/10.1063/1.4929852
View Table of Contents: http://scitation.aip.org/content/aip/journal/pop/22/9?ver=pdfcov
Published by the AIP Publishing

Quasilinear saturation of the aperiodic ordinary mode streaming instability

A. Stockem Novo,[1,a)] P. H. Yoon,[2,3] M. Lazar,[1,4] R. Schlickeiser,[1] S. Poedts,[4] and J. Seough[5,6]
[1]*Institut für Theoretische Physik, Lehrstuhl IV: Weltraum-und Astrophysik, Ruhr-Universität Bochum, D-44780 Bochum, Germany*
[2]*Institute for Physical Science & Technology, University of Maryland, College Park, Maryland 20742, USA*
[3]*School of Space Research, Kyung Hee University, Yongin-Si, Gyeonggi-Do 446-701, Korea*
[4]*Centre for Mathematical Plasma Astrophysics, Celestijnenlaan 200B, 3001 Leuven, Belgium*
[5]*Faculty of Human Development, University of Toyama, 3190, Gofuku, Toyama City, Toyama 930-8555, Japan*
[6]*International Research Fellow of the Japan Society for the Promotion of Science, Tokyo, Japan*

(Received 19 June 2015; accepted 11 August 2015; published online 2 September 2015)

In collisionless plasmas, only kinetic instabilities and fluctuations are effective in reducing the free energy and scatter plasma particles, preventing an increase of their anisotropy. Solar energetic outflows into the interplanetary plasma give rise to important thermal anisotropies and counterstreaming motions of plasma shells, and the resulting instabilities are expected to regulate the expansion of the solar wind. The present paper combines quasilinear theory and kinetic particle-in-cell simulations in order to study the weakly nonlinear saturation of the ordinary mode in hot counter-streaming plasmas with a temperature anisotropy as a follow-up of the paper by Seough *et al*. [Phys. Plasmas **22**, 082122 (2015)]. This instability provides a plausible mechanism for the origin of dominating, two-dimensional spectrum of transverse magnetic fluctuations observed in the solar wind. Stimulated by the differential motion of electron counterstreams the O mode instability may convert their free large-scale energy by nonlinear collisionless dissipation on plasma particles. © *2015 AIP Publishing LLC*. [http://dx.doi.org/10.1063/1.4929852]

I. INTRODUCTION

Interpenetrating bi-directional streams of electrons and ions are frequently observed in space plasmas, e.g., during coronal mass ejections (CMEs)[2,3] or associated with the interplanetary shocks, including the Earth's bow shock[4] and corotating interaction regions (CIRs),[5,6] as well as depletions of halo particles around 90° pitch-angle at reverse shocks.[7] Counter-streaming plasmas may be subject to a variety of electrostatic and electromagnetic instabilities driven by the differential streaming and the temperature anisotropy of these plasmas. Among them, the ordinary mode (O mode) instability is presently receiving a renewed increasing interest[8–14,16] mainly triggered by its potential relevance in space plasma applications, e.g., as a physical mechanism for the origin of dominating, two-dimensional transverse magnetic fluctuation spectrum in the solar wind.[17]

In the absence of streaming plasmas, the O mode instability is driven by an excess of parallel temperature $T_\parallel > T_\perp$, where $\parallel, \perp$ denote directions with respect to the regular magnetic field $\mathbf{B}_0$, and for perpendicular propagation ($\mathbf{k} \perp \mathbf{B}_0$), it is decoupled from other plasma modes,[8,9,11,18] resembling features of the aperiodic Weibel instability[20] in unmagnetized plasmas. The O-mode instability is stimulated by additional streaming of plasma particles along $\mathbf{B}_0$,[21–27] making it more effective but also more intriguing in the competition with other instabilities.[16,27,28] From linear theory, we can compare the instability thresholds and characterize the fastest growing modes, but from the nonlinear evolution of the resulting fluctuations, their effects on plasma particles can be understood. Growing fluctuations may effectively interact with plasma particles, reducing their anisotropy and leading to the instability saturation.[29] These effects can be identified and quantified by a quasilinear analysis of the growing modes and their back-reaction on the particle distribution functions.[30–32]

In a companion paper,[1] the quasilinear relaxation of the classic O mode instability driven by initial bi-Maxwellian distribution of electrons was investigated. In order to validate the theory, the particle-in-cell simulation was also carried out with one-dimensional (1D) spatial coordinate and three-dimensional (3D) velocity space. To complete the quasilinear analysis performed in the companion paper[1] for the O mode instability in non-streaming plasmas, in this paper, we propose to examine the weakly nonlinear saturation of this instability in hot counter-streaming plasmas with a temperature anisotropy. The development of the O mode streaming instability is considered in symmetric counter-streaming plasmas (when the O mode is decoupled from the extraordinary mode) by means of the quasilinear kinetic theory as well as the particle-in-cell (PIC) simulations.

II. LINEAR DISPERSION RELATION FOR ORDINARY MODE INSTABILITY

The general linear dispersion relation for the O mode is given by[8,9,11,18]

$$\omega^2 = c^2 k_\perp^2 + \sum_a \omega_{pa}^2 \left[1 + \sum_{n=1}^{\infty} \frac{2n^2\Omega_a^2}{n^2\Omega_a^2 - \omega^2} \times \int d\mathbf{v}\, J_n^2\left(\frac{k_\perp v_\perp}{\Omega_a}\right) \frac{v_\parallel^2}{v_\perp} \frac{\partial f_a}{\partial v_\perp} \right], \quad (1)$$

where $\int d\mathbf{v} = 2\pi \int_{-\infty}^{\infty} dv_\parallel \int_0^\infty dv_\perp v_\perp$; subscript a stands for particle species ($a = e$ for electrons and $a = p$ for protons);

[a)]Electronic address: anne@tp4.rub.de.

$k_\perp$ is the wave number perpendicular to the ambient magnetic field; $\omega_{pa} = (4\pi e_a^2 n_0/m_a)^{1/2}$ is the plasma frequency for species a, n_0 being the ambient plasma density, e_a and m_a being the unit electric charge and mass for particle species a; $\Omega_a = e_a B_0/m_a c$ is the cyclotron frequency for species a, B_0 the ambient magnetic field intensity, and c being the speed of light *in vacuo*; $J_n(x)$ is the Bessel function of first kind; and f_a is the particle velocity distribution function normalized to unity, $\int d\mathbf{v} f_a = 1$. As in the companion paper[1] we consider the electron response only, but unlike Ref. 1 where we implicitly assumed that the parallel component of the electron velocity distribution function is Maxwellian, we now consider the counter-streaming parallel distribution function. Note that the formalism in Ref. 1 does not depend on the detailed form of the parallel distribution, as long as the total velocity distribution can be expressed as a product of the reduced parallel and perpendicular distributions

$$f(\mathbf{v}) = F(v_\perp)G(v_\parallel), \tag{2}$$

where the species subscripts $a = e$ have been omitted. The parallel distribution $G(v_\parallel)$ is an arbitrary smooth function normalized according to $\int_{-\infty}^{\infty} dv_\parallel G(v_\parallel) = 1$. Since in Ref. 1 the bulk velocity is zero, $V = 0$, the effective parallel temperature was defined simply as

$$T_\parallel^{\text{eff}} = m\int_{-\infty}^{\infty} dv_\parallel\, v_\parallel^2 G(v_\parallel), \tag{3}$$

which does not depend on the detailed mathematical form of $G(v_\parallel)$. As in Ref. 1, the perpendicular distribution $F(v_\perp)$ is assumed to be given by the Maxwellian form

$$F(v_\perp) = \frac{m}{2\pi T_\perp}\exp\left(-\frac{mv_\perp^2}{2T_\perp}\right), \tag{4}$$

where the perpendicular temperature $T_\perp$ is defined by the second velocity moment, $T_\perp = \pi m\int_0^\infty dv_\perp v_\perp^3 F(v_\perp)$.

In the present paper, we are now interested in the counter-streaming parallel distribution

$$G(v_\parallel) = \frac{1}{2}\left(\frac{m}{2\pi T_\parallel}\right)^{1/2}\left[\exp\left(-\frac{m(v_\parallel+V)^2}{2T_\parallel}\right) + \exp\left(-\frac{m(v_\parallel-V)^2}{2T_\parallel}\right)\right], \tag{5}$$

where we define the parallel "temperature" in terms of the Gaussian velocity spread associated with each component and $\pm V$ is the bulk velocity. This is more meaningful since space when two or more drifting populations of plasmas are measured, the "temperature" is often defined in association with each population. Had we simply defined the "effective" temperature via Eq. (3), then we would obtain the relationship between $T_\parallel^{\text{eff}}$ and $T_\parallel$ as well as the counter-streaming average speed

$$T_\parallel^{\text{eff}} = T_\parallel + mV^2. \tag{6}$$

Henceforth, we do not consider $T_\parallel^{\text{eff}}$, but we treat $T_\parallel$ as the parallel temperature, and treat V as a separate input parameter.

With the model distribution (2), (4), and (5), it is straightforward to obtain the O mode dispersion relation[11–14,16]

$$c^2k_\perp^2 = \omega^2 - \omega_{pe}^2\left(1 - \frac{T_\parallel + mV^2}{T_\perp}\sum_{n=1}^{\infty}\frac{2n^2\Omega_e^2\Lambda_n(\lambda)}{n^2\Omega_e^2 - \omega^2}\right), \tag{7}$$

with $\lambda = \frac{k_\perp^2 T_\perp}{m\Omega_e^2}$ and $\Lambda_n(\lambda) = I_n(\lambda)e^{-\lambda}$. In the above $I_n(x)$ is the n^{th} order modified Bessel function of first kind. Note that Eq. (7) is structurally identical to the dispersion relation for classical O-mode instability for bi-Maxwellian case,[18] if we simply replace $T_\parallel + mV^2$ by $T_\parallel^{\text{eff}}$. However, as we argued above, treating the total thermal plus counter-streaming beam energy as a net effective temperature is not necessarily the most informative way, as space observations often distinguish the thermal spread and beam energy separately.[19] The necessary condition for the aperiodic, that is, purely growing unstable solution, where the real part of the frequency is zero, $\omega_r = 0$, and the imaginary part is positive, $\gamma > 0$, is

$$1 - \frac{T_\perp}{T_\parallel} > \frac{2\lambda}{\beta_\parallel} + \Lambda_0(\lambda) - \frac{mV^2}{T_\parallel}\left[1 - \Lambda_0(\lambda)\right]. \tag{8}$$

Here, $\beta_\parallel = 8\pi n_0/T_\parallel$ is the parallel electron beta defined in terms of the Gaussian thermal spread. Note that Eq. (8) is a direct generalization of the similar condition discussed in Ref. 18. In the case of classic O-mode instability without the counter-streaming feature, the marginal stability condition can be numerically determined by requiring that the factor $1 - T_\perp/T_\parallel$ be higher than minimum value of the function $G(\lambda) = 2\lambda/\beta_\parallel + \Lambda_0(\lambda)$, treating $\beta_\parallel$ as a free input parameter. In the case of counter-streaming feature, an additional quantity V becomes another free input parameter. Nevertheless, Eq. (8) can be numerical analyzed in a similar way. Note that Ref. 14 analytically solved the above marginal stability condition in order to obtain the empirical closed-form relationship between $T_\perp/T_\parallel$ and $\beta_\parallel$. In the present paper, we determine the exact threshold condition by manipulating Eq. (8) by numerical means.

Figure 1 shows the O-mode dispersion relation for input parameters $(\omega_{pe}/\Omega_e)^2 = 50$, $T_\perp/T_\parallel = 0.2$, $\beta_\parallel = 3$ and four different normalized counter-streaming electron beam speeds

$$P \equiv \frac{4\pi n_0 mV^2}{B_0^2} = 0, 0.5, 1, 1.5. \tag{9}$$

The blue curves correspond to the real frequency, $\text{Re}(\omega/\Omega)$, while the red curves depict the growth rate $\text{Im}(\omega/\Omega)$. The horizontal axis is the normalized perpendicular wave number λ in logarithmic scale. The first case (top-left) of $P = 0$ correspond to the classic bi-Maxwellian situation. For this case, the O-mode is stable. The second case (top-right) with $P = 0.5$ shows that the first harmonic cyclotron mode and the zeroth order mode begin to move toward each other, but the instability threshold has not been crossed yet, and the system is still stable. For $P = 1$ (bottom-left), the first harmonic mode and the zeroth order mode have now merged to form a pair of complex conjugate solutions (instability). Finally, the bottom-right panel shows the case of $P = 1.5$ where the O mode instability growth has increased and the range of unstable λ has

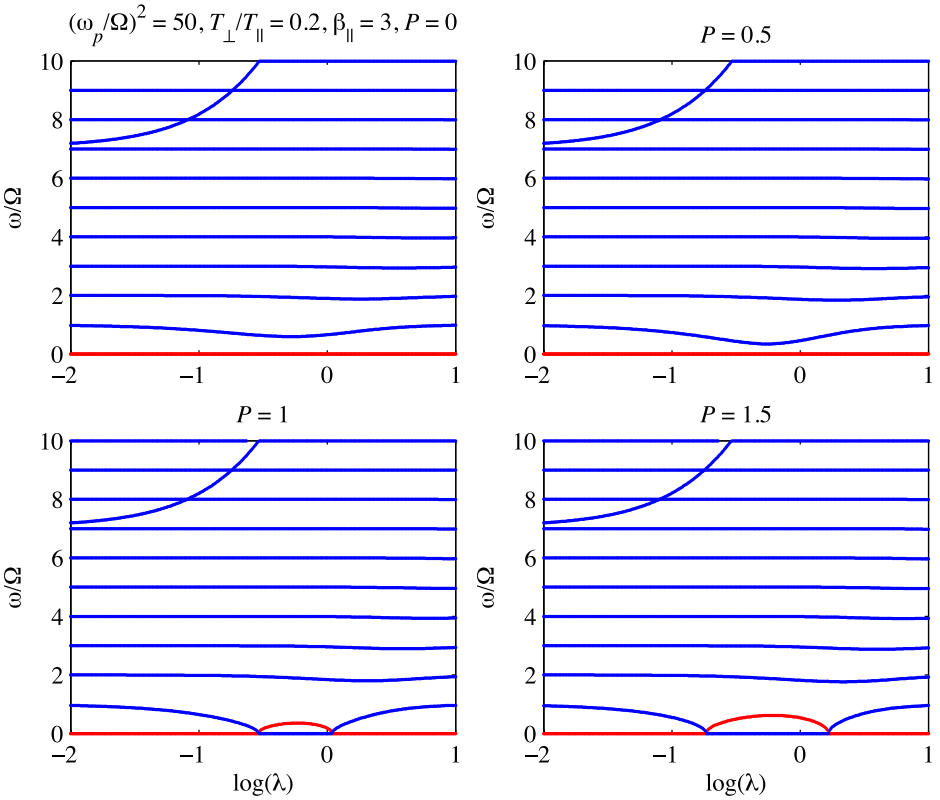

FIG. 1. The real frequency $\mathrm{Re}(\omega/\Omega)$ (blue) and growth rate $\mathrm{Im}(\omega/\Omega)$ (red) for the O mode versus normalized wave number $\lambda = k_\perp^2 T_\perp/(m\Omega_e^2)$ in logarithmic scale, for $\omega_{pe}^2/\Omega^2 = 50$, $T_\perp/T_\parallel = 0.2$, for $\beta_\parallel = 3$ and for $P = 0$, 0.5, 1, and 1.5.

increased. Note also that the fast ordinary mode dispersion relation, $\omega^2 = \omega_{pe}^2 + c^2k_\perp^2$ is intersected by ordinary-Bernstein mode at each harmonic.[15] The cutoff frequency for the fast O mode is $\omega_O = \omega_{pe}$. The value of the frequency ratio $(\omega_{pe}/\Omega_e)^2$, which in this case is 50, generally has very little influence on the O mode instability. For higher ratio, the cutoff frequency associated with the fast O mode simply moves to higher frequency, until the fast O mode moves out of the vertical plotting range, yet the aperiodic O-mode instability remains the same.

Figure 2 plots the maximum growth rate for the aperiod unstable branch (corresponding to $n = 0$ harmonic mode) over the phase space $(\beta_\parallel, T_\perp/T_\parallel)$ for $(\omega_{pe}/\Omega_e)^2 = 200$, together with the contours of constant maximum growth rate $\gamma_{\max}/\Omega$. The red curve is the marginal stability condition computed from Eq. (8) by numerical means, which is a direct generalization of

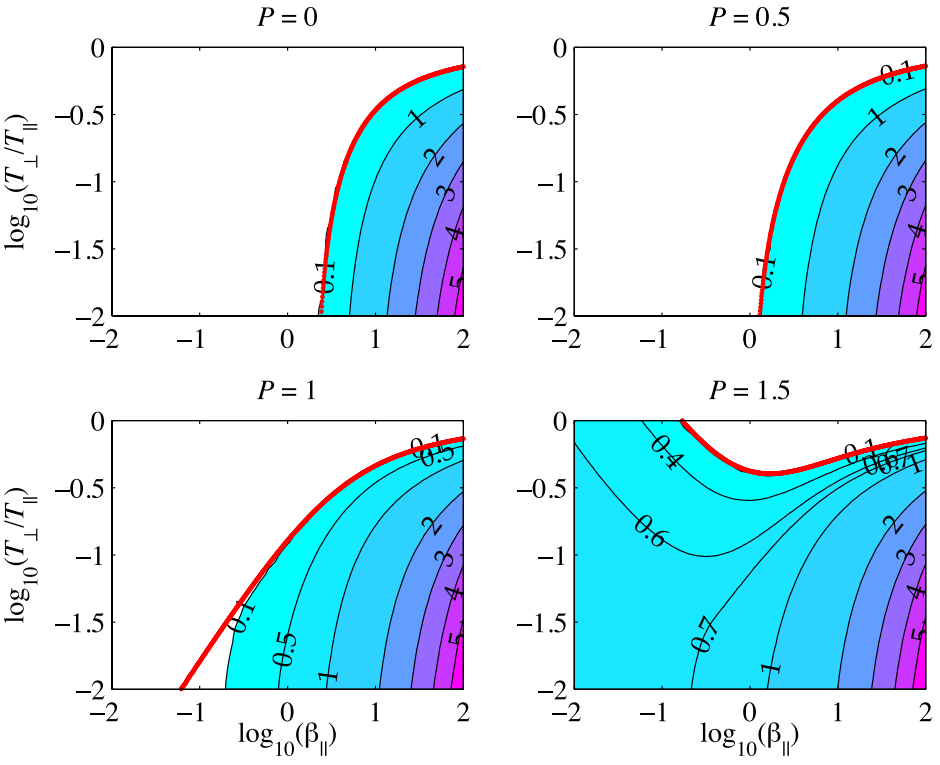

FIG. 2. The plot (with colormap) of the maximum growth rate superposed with the constant $\gamma_{\max}/\Omega$ contours in two-dimensional space $(\beta_\parallel, T_\perp/T_\parallel)$, for $(\omega_{pe}/\Omega)^2 = 200$.

the threshold condition found in Ref. 18. In fact, the case of $P=0$ corresponds exactly the same as that of Ref. 18. For $P=0.5$, Figure 2 shows that the marginal stability boundary is only moderately changed. When P increases to 1, the marginal stability boundary is visibly modified, covering a wider region in $(\beta_\parallel, T_\perp/T_\parallel)$ space. For $P=1.5$, the unstable region becomes much wider and covers a significant portion of the low $\beta_\parallel$ region. Such a behavior was first noted in Refs. 11 and 12.

We next consider the nonlinear behavior of the O mode instability. We investigate the dynamic development and saturation by means of quasilinear theory and particle-in-cell simulation.

III. QUASILINEAR THEORY OF ORDINARY MODE STREAMING INSTABILITY

-mode streaming instability in the linear phase of exponential growth is driven by the counter-streaming bi-Maxwellian distribution of electrons, but once the system evolves beyond the linear stage, the electron velocity distribution is expected to deviate from the strict counter-streaming bi-Maxwellian form. However, in order to facilitate the quasilinear analysis, let us make an assumption that the electron distribution retains the same mathematical form as the initial distribution, except that the temperatures and the streaming velocity adiabatically evolves

$$f=\frac{1}{2}\frac{m^{3/2}}{(2\pi)^{3/2}T_\perp(t)T_\parallel^{1/2}(t)}\exp\left(-\frac{mv_\perp^2}{2T_\perp(t)}\right)\times\left[\exp\left(-\frac{m\left[v_\parallel+V(t)\right]^2}{2T_\parallel(t)}\right)+\exp\left(-\frac{m\left[v_\parallel-V(t)\right]^2}{2T_\parallel(t)}\right)\right]. \tag{10}$$

Of course, this is an approximation, and we will check the validity of this approximation against the particle-in-cell simulation. In quasilinear approximation, nonlinear mode coupling is ignored, and the wave kinetic equation (for the magnetic perturbation) is simply given by

$$\frac{\partial\delta B^2}{\partial t}=2\gamma\,\delta B^2, \tag{11}$$

and the instantaneous dispersion relation is given by Eq. (7).

In the companion paper,[1] we derived the quasilinear evolution equation for the second velocity moments, so that we may make use of the results found there, except that instead of interpreting the second parallel velocity moment as the parallel temperature, we now have

$$\begin{aligned}\frac{dT_\perp}{dt}&=\frac{d}{dt}\frac{m}{2}\int d\mathbf{v}v_\perp^2 f\\&=\frac{2\pi e^2}{mc^2}\int_0^\infty\frac{dk_\perp}{k_\perp}\gamma\delta B^2\left(1+\frac{c^2k_\perp^2}{\omega_{pe}^2}+\frac{\gamma^2}{\omega_{pe}^2}\right),\\\frac{dT_\parallel}{dt}+m\frac{dV^2}{dt}&=\frac{d}{dt}m\int d\mathbf{v}v_\parallel^2 f\\&=\frac{4\pi e^2}{mc^2}\int_0^\infty\frac{dk_\perp}{k_\perp}\gamma\delta B^2\left[1-2\left(1+\frac{c^2k_\perp^2}{\omega_{pe}^2}+\frac{\gamma^2}{\omega_{pe}^2}\right)\right].\end{aligned} \tag{12}$$

Apparently, $T_\parallel$ and V^2 are coupled in the second equation of Eq. (12). We need another equation to decouple the two quantities. The third-order moment $\int d\mathbf{v}v_\parallel^3 f$ is zero since the distribution (10) is symmetric with respect to $v_\parallel$. We thus consider the fourth moment

$$\int d\mathbf{v}v_\parallel^4 f=\frac{3T_\parallel^2}{m^2}+\frac{6T_\parallel V^2}{m}+V^4. \tag{13}$$

On the other hand, from the quasilinear velocity space diffusion equation discussed in Ref. 1

$$\begin{aligned}\frac{\partial f}{\partial t}=&\frac{2\pi ie^2}{m^2c^2}\sum_{n=-\infty}^{\infty}\int_0^\infty\frac{dk_\perp}{k_\perp}\delta B^2(k_\perp)\\&\times\left(n\Omega_e\frac{v_\parallel}{v_\perp}\frac{\partial}{\partial v_\perp}-(i\gamma+n\Omega_e)\frac{\partial}{\partial v_\parallel}\right]\\&\times J_n^2\left(\frac{k_\perp v_\perp}{\Omega_e}\right)\left(\frac{n\Omega_e}{i\gamma-n\Omega_e}\frac{v_\parallel}{v_\perp}\frac{\partial f}{\partial v_\perp}+\frac{\partial f}{\partial v_\parallel}\right),\end{aligned} \tag{14}$$

and the dispersion relation (7) it is possible to derive

$$\begin{aligned}m^2\int d\mathbf{v}v_\parallel^4\frac{\partial f}{\partial t}=&-\frac{8\pi e^2}{c^2}\frac{m}{T_\parallel+mV^2}\int_0^\infty\frac{dk_\perp}{k_\perp}\gamma\delta B^2(k_\perp)\\&\times\left[2\left(\frac{3T_\parallel^2}{m^2}+\frac{6T_\parallel V^2}{m}+V^4\right)\right.\\&\left.\times\left(1+\frac{\gamma^2}{\omega_{pe}^2}+\frac{c^2k_\perp^2}{\omega_{pe}^2}\right)-3\left(\frac{T_\parallel}{m}+V^2\right)^2\right].\end{aligned} \tag{15}$$

By combining Eqs. (13) and (15), we may now decouple the evolution equation for $T_\parallel$ and V^2 in the second equation of Eq. (12)

$$\begin{aligned}\frac{dV^2}{dt}=&-\frac{8\pi e^2}{mc^2}\frac{V^2}{T_\parallel+mV^2}\int_0^\infty\frac{dk_\perp}{k_\perp}\gamma\delta B^2(k_\perp)\\&\times\left(1+\frac{\gamma^2}{\omega_{pe}^2}+\frac{c^2k_\perp^2}{\omega_{pe}^2}\right),\\\frac{dT_\parallel}{dt}=&-m\frac{dV^2}{dt}+\frac{4\pi e^2}{mc^2}\int_0^\infty\frac{dk_\perp}{k_\perp}\gamma\delta B^2(k_\perp)\\&\times\left[1-2\left(1+\frac{\gamma^2}{\omega_{pe}^2}+\frac{c^2k_\perp^2}{\omega_{pe}^2}\right)\right].\end{aligned} \tag{16}$$

We have solved the equations for $T_\perp$, V^2, and $T_\parallel$—the first equation in Eqs. (12) and (16)—for the initial condition specified by $\omega_{pe}^2/\Omega_e^2=200$, $\beta_\parallel=5$, $T_\perp/T_\parallel=0.05$, and for two different counter-streaming beam speeds, $V/c=0.05$ and 0.07, which in terms of the dimensionless quantity P defined in Eq. (9), is equivalent to $P=0.5$ and 1. We will defer the presentation of the quasilinear analysis until we discuss the particle-in-cell (PIC) simulation result, where a direct comparison with the quasilinear analysis will be made. In Sec. IV, we first discuss the PIC simulation methodology and setup.

IV. PARTICLE-IN-CELL SIMULATION

In order to test the theory, we perform kinetic particle-in-cell simulations with the fully relativistic code

OSIRIS.[33–35] We use a one-dimensional simulation box which is oriented perpendicular to the counter-streaming beams of electrons to exclude competing perpendicular modes. Two populations of electrons are interpenetrating each other with initial streaming velocities $v_0/c = \pm 0.05$ (run 1) and $v_0/c = \pm 0.07$ (run 2) and temperature anisotropy $A = T_\perp/T_\parallel = 0.01$ with $v_{th,||} = 0.158c$. The protons are forming a neutralizing background with zero fluid velocity and thermal velocity $v_{th} = 8.2 \times 10^{-4}c$. The ambient magnetic field is aligned with the beams and thus perpendicular to the simulation direction with electron gyro frequency $\Omega_e/\omega_{pe} = 0.0707$.

We use periodic boundary conditions for the particles and fields. The simulation box has a length of $L = 102.4\, c/\omega_{pe}$ with a spatial resolution $\Delta x = 0.1\, c/\omega_{pe} = 7.5 \times 10^{-3} c/\Omega_e$ and 100 particles per cell and species using a cubic interpolation scheme. The temporal resolution is $\Delta t = 0.0752\, \omega_{pe}^{-1} = 5.3 \times 10^{-3}\, \Omega_e$. We also performed tests with higher spatial resolution in order to make sure that the resolution is sufficient.

V. NUMERICAL ANALYSIS INCLUDING COMPARISON BETWEEN QUASILINEAR THEORY AND PIC SIMULATION

In this section, we now discuss the results of numerical analysis based upon the quasilinear method in conjunction with the PIC simulation results.

The perpendicular mode gives rise to an initially exponentially growing magnetic field (Fig. 3), which is saturated for later times. Figure 4 shows a good match between the simulations and quasi-linear theory. The exponential growth and the time of saturation at $\approx 5\, \Omega_e^{-1}$ are well described by theory. The saturation field is slightly underestimated by 6–10%.

The same holds for the parallel fluid velocity shown in Fig. 5. The drop from the initial value v_0/c is well described while the saturation value is slightly overestimated by theory with a deviation of 10%. This is probably due to the fact that the electron distributions in the simulations deviate from a perfect Maxwellian. The oscillations are an effect of the 1D-simulation and do not appear in 2D.

The evolution of the parallel and perpendicular plasma beta matches only qualitatively; see Fig. 6 with a strong deviation of up to 20%. The saturation value of $\beta_\parallel \approx 3$ is the same for both runs. Since $\beta_\parallel$ and $\beta_\perp$ are defined by the

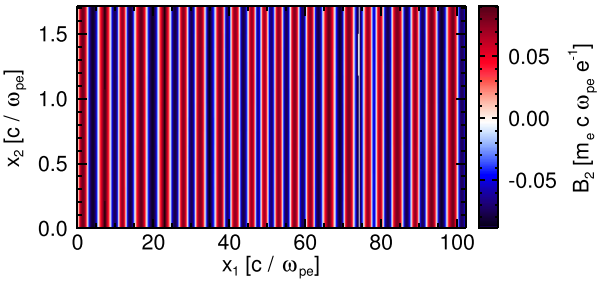

FIG. 3. Perpendicular magnetic field in the simulation plane at $t\Omega_e = 35$ for $v_0/c = \pm 0.05$.

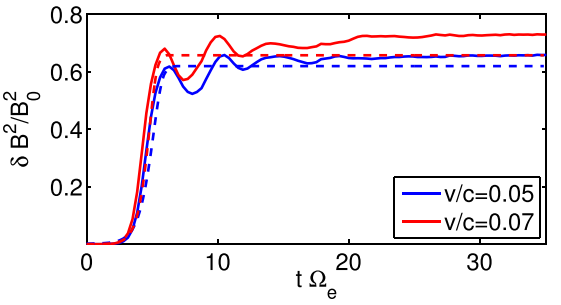

FIG. 4. Normalized perturbative magnetic field energy versus time for different initial streaming velocities from simulations (solid) and QL theory (dashed).

temperature, a non-Maxwellian shape of the electron distribution function might sensitively affect this value.

VI. SUMMARY

Following up on Seough *et al.*,[1] we have studied the saturation of the ordinary mode instability in hot counter-streaming plasmas with a temperature anisotropy. We have looked at a collisionless plasma of electrons and protons, where the latter form a neutralizing background. Two counter-streaming electron populations were considered with a temperature anisotropy and the direction of higher temperature being aligned with an ambient magnetic field.

Starting from initially bi-Maxwellian distributions, a stability criterion has been derived, which allows for the determination of a maximum growth rate of the O-mode instability. Furthermore, using the assumption that the modified electron distributions at later times can still be modeled by bi-Maxwellian distributions, the temporal evolution of the magnetic field perturbations, the parallel and perpendicular temperatures and the particle distribution function could be derived in a self-consistent treatment.

The analytical results have been compared against kinetic particle-in-cell simulations, which were performed in a one-dimensional setup in order to exclude interfering modes. A qualitative good agreement was found between both methods. The exponentially growing phase and time of saturation can be well predicted by the theory, while the saturation value differs by 10% for the magnetic field fluctuations and

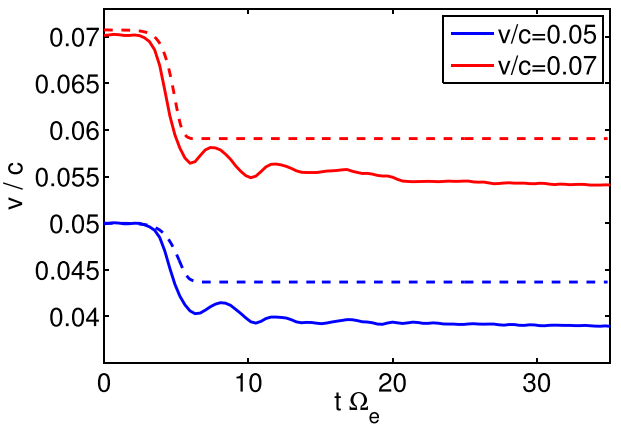

FIG. 5. Parallel velocity versus time for different initial streaming velocities from simulations (solid) and QL theory (dashed).

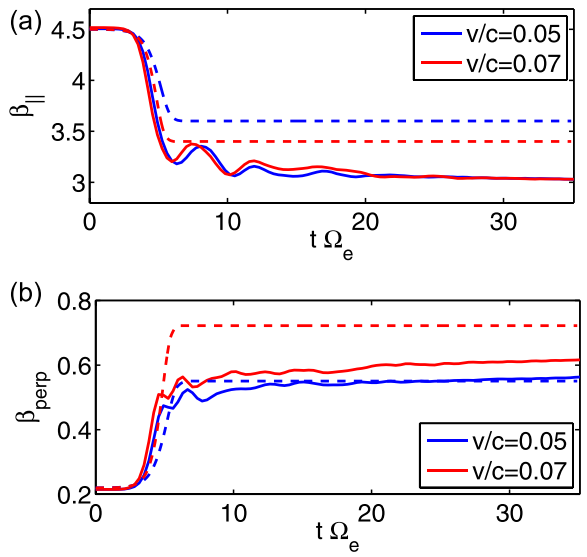

FIG. 6. Parallel and perpendicular plasma beta versus time for different initial streaming velocities from simulations (solid) and QL theory (dashed).

average velocity. The deviation of up to 20% for parallel and perpendicular plasma betas is probably due to the fact that the distribution functions are not perfect Maxwellians, which were used in the analytical approach.

In conclusion, we found a self-consistent and robust model to describe the non-linear saturation of the O mode instability. This instability is found to be quite effective in isotropizing the temperature as well as the counter-streams, redistributing the free energy and heating plasma particles. To improve the analysis quantitatively, a numerical modeling of the actual distribution function has to be used.

ACKNOWLEDGMENTS

P.H.Y. acknowledges NSF Grant Nos. AGS1138720 and AGS1242331 to the University of Maryland, and the BK21-Plus grant to Kyung Hee University, Korea, from the National Research Foundation (NRF) funded by the Ministry of Education of Korea. Part of this work was carried out while P.H.Y. was visiting Ruhr University Bochum, Germany, which was made possible by support from the Ruhr University Research School PLUS, funded by Germany's Excellence Initiative (DFG GSC 98/3). The work of R.S. was supported by the Deutsche Forschungsgemeinschaft through grant Schl 201/32-1. M.L. acknowledges support from the KU Leuven, Grant No. SF/12/003, and from the Ruhr-Universität Bochum. These results were obtained in the framework of the Project Nos. GOA/2015-014 (KU Leuven) and C 90347 (ESA Prodex 9). For the computations we used the infrastructure of the VSC Flemish Supercomputer Center, funded by the Hercules foundation and the Flemish Government department EWI. J.S. acknowledges the Postdoctoral fellowship for Foreign Researchers of the Japan Society for the Promotion of Science (Grant No. P14028). The authors would like to acknowledge the OSIRIS Consortium, consisting of UCLA and IST (Lisbon, Portugal) for the use of OSIRIS, for providing access to the OSIRIS 3.0 framework. We also acknowledge the Gauss Centre for Supercomputing (GCS) for providing computing time through the John von Neumann Institute for Computing (NIC) on the GCS share of the supercomputer JUQUEEN at Jülich Supercomputing Centre (JSC) and the Thinking cluster at KU Leuven.

[1]J. Seough, P. H. Yoon, J. Hwang, and Y. Nariyuki, Phys. Plasmas **22**, 082122 (2015).
[2]B. R. Anderson, R. M. Skoug, J. T. Steinberg, and D. J. McComas, J. Geophys. Res. **117**, A04107, doi:10.1029/2011JA017269 (2012).
[3]M. Lazar, J. Pomoell, S. Poedts, C. Dumitrache, and N. A. Popescu, Solar Phys. **289**, 4239 (2014).
[4]W. C. Feldman, J. R. Asbridge, S. J. Bame, and M. D. Montgomery, Rev. Geophys. Space Phys. **12**, 715, doi:10.1029/RG012i004p00715 (1974).
[5]J. T. Steinberg, J. T. Gosling, R. M. Skoug, and R. C. Wiens, J. Geophys. Res. **110**, A06103, doi:10.1029/2005JA011027 (2005).
[6]J. T. Gosling, S. J. Bame, W. C. Feldman, D. J. McComas, J. L. Phillips, and B. E. Goldstein, Geophys. Res. Lett. **20**, 2335, doi:10.1029/93GL02489 (1993).
[7]R. M. Skoug, J. T. Gosling, D. J. McComas, C. W. Smith, and Q. Hu, J. Geophys. Res. **111**, A01101, doi:10.1029/2005JA011316 (2006).
[8]S. Hamasaki, Phys. Fluids **11**, 1173 (1968).
[9]S. Hamasaki, Phys. Fluids **11**, 2724 (1968).
[10]A. Stockem, I. Lerche, and R. Schlickeiser, Astrophys. J. **651**, 584 (2006).
[11]D. Ibscher, M. Lazar, and R. Schlickeiser, Phys. Plasmas **19**, 072116 (2012).
[12]D. Ibscher, M. Lazar, M. J. Michno, and R. Schlickeiser, Phys. Plasmas **20**, 012103 (2013).
[13]F. Hadi, M. F. Bashir, A. Qamar, P. H. Yoon, and R. Schlickeiser, Phys. Plasmas **21**, 052111 (2014).
[14]R. Schlickeiser and P. H. Yoon, Phys. Plasmas **21**, 072119 (2014).
[15]C. Z. Cheng, J. Plasma Phys. **13**, 335 (1975).
[16]M. Lazar, R. Schlickeiser, S. Poedts, and S. Vafin, Phys. Plasmas **22**, 012102 (2015).
[17]O. Alexandrova, C. H. K. Chen, L. Sorriso-Valvo, T. S. Horbury, and S. D. Bale, Space Sci. Rev. **178**, 101 (2013).
[18]R. C. Davidson and C. S. Wu, Phys. Fluids **13**, 1407 (1970).
[19]A. F. Viñas, C. Gurgiolo, T. Nieves-Chinchilla, S. P. Gary, and M. L. Goldstein, AIP Conf. Proc. **1216**, 265 (2010).
[20]E. S. Weibel, Phys. Rev. Lett. **2**, 83 (1959).
[21]H. P. Furth, Phys. Fluids **6**, 48 (1963).
[22]K. F. Lee, Phys. Rev. **181**, 447 (1969).
[23]K. F. Lee, J. Appl. Phys. **41**, 3045 (1970).
[24]M. Bornatici and K. F. Lee, Phys. Fluids **13**, 3007 (1970).
[25]K. F. Lee and J. C. Armstrong, Phys. Rev. A **4**, 2087 (1971).
[26]J. D. Gaffey, W. B. Thompson, and C. S. Liu, J. Plasma Phys. **7**, 189 (1972).
[27]W. M. Chen and C. S. Lai, Phys. Fluids **16**, 277 (1973).
[28]B. Buti, Astrophys. J. **181**, 1055 (1973).
[29]R. C. Davidson, *Methods in Nonlinear Plasma Theory* (Academy Press, New York, 1972).
[30]R. C. Davidson, D. A. Hammer, I. Haber, and C. E. Wagner, Phys. Fluids **15**, 317 (1972).
[31]P. H. Yoon, Phys. Fluids B **3**, 3074 (1991).
[32]P. H. Yoon, J. J. Seough, K. H. Kim, and D. H. Lee, J. Plasma Phys. **78**, 47 (2012).
[33]R. A. Fonseca, L. O. Silva, F. S. Tsung, V. K. Decyk, W. Lu, C. Ren, W. B. Mori, S. Deng, S. Lee, T. Katsouleas, and J. C. Adam, Lecture Notes Comput. Sci. **2331**, 342 (2002).
[34]R. A. Fonseca, S. F. Martins, L. O. Silva, J. W. Tonge, F. S. Tsung, and W. B. Mori, Plasma Phys. Controlled Fusion **50**, 124034 (2008).
[35]R. A. Fonseca, J. Vieira, F. Fiuza, A. Davidson, F. S. Tsung, W. B. Mori, and L. O. Silva, Plasma Phys. Controlled Fusion **55**, 124011 (2013).